Using Rogowski Coils Inside Protective Relays

Veselin Skendzic and Bob Hughes, *Schweitzer Engineering Laboratories, Inc.*

***Abstract*—Traditionally, microprocessor-based relays incorporate a secondary current transformer to convert the 5 A or 1 A input current to a lower level for input to an analog-to-digital (A/D) converter as part of the input processing. The limits of this input circuit are well known, and relay designers take them into account when determining operating characteristics.**

A Rogowski coil produces an output based on the rate of change of the current input, so passing the output of the coil through an integrator produces a signal that is proportional to the current. There are additional characteristics of a Rogowski coil that give it particular advantages for use in a microprocessor-based relay, including the following:

- **An air core. This leads to no saturation, even at very high currents.**
- **A flexible shape. With no iron core, the coil can be shaped and sized to fit the application.**
- **Immunity to electromagnetic interference. This makes the coil suitable for electrically noisy environments.**

These advantages, and others, make a Rogowski coil something to consider for the input of microprocessor-based relays, where the integration required to obtain the input current is a relatively easy operation. This paper discusses the practical considerations of using this coil in a relay. Complicating and mitigating factors are discussed, along with the performance impact on the relay and practical experiences in the field.

Application impacts of Rogowski coil use are presented, including which types of relays are most benefited by this technology. Future implications of this technology are also presented.

I. Introduction

Rogowski coil technology is well known in the power industry. Its origins can be traced back to 1912, but at that time, the low-energy coil output and the fact that it measures the derivative of the input current made it impractical for use with the prevailing electromechanical relay technology [1]. Practical applications of Rogowski coil-based technology have been steadily rising, but the rate of adoption remains slow, mostly owing to the excellent performance, high reliability, and low cost delivered by conventional current transformers (CTs).

With the advent of modern microprocessors, Rogowski coils are gaining additional momentum and are being slowly brought into everyday applications. Based on their operating principle, Rogowski coils are closely related to linear couplers (air core mutual inductors), which have earned their place in the most demanding high-current applications, such as arc-furnace transformer or low-voltage busbar protection applications.

The primary difference between conventional CTs, linear couplers, and Rogowski coils can be summarized as follows: Conventional CTs are insensitive to the position of the primary conductor inside the core and provide exceptional rejection of external magnetic fields, but the core can saturate under high-current fault conditions (including dc offset). Linear couplers do not saturate but are sensitive to external magnetic fields and the primary conductor position. Similar to linear couplers, Rogowski coils do not saturate, but they also include well-controlled geometry with a return loop, which improves external magnetic field rejection and makes the coil less sensitive to the primary conductor position.

Rogowski coils are well recognized as primary current sensors and are exceptionally well suited for applications where high-voltage insulation is provided by the adjoining apparatus, such as in gas-insulated switchgear, dead-tank high-voltage breakers, medium-voltage applications (as shown in Fig. 1), and low-voltage applications.

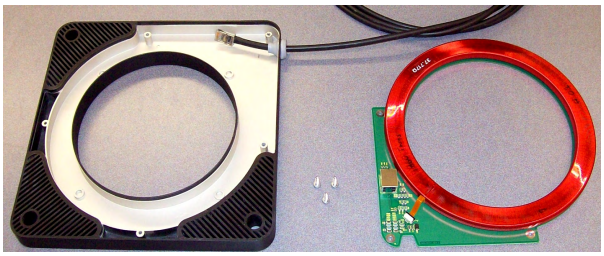

Fig. 1. Medium-voltage Rogowski coil design example.

The use of Rogowski coils in the CT secondary circuits is less known and is documented in this paper with the samples shown in Fig. 2.

Fig. 2. Conventional CT and the Rogowski coils with conventional CT components in the middle (core, core with secondary, and completed CT assembly).

II. Theory of Operation

References [1] and [2] provide excellent tutorials on the Rogowski coil theory of operation. For the purposes of this paper, it is sufficient to know that the coil produces voltage output proportional to the derivative of the current enclosed by the coil contour. The physical arrangement is illustrated in Fig. 3.

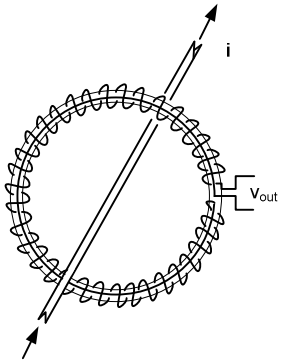

Fig. 3. Rogowski coil current sensor.

Voltage induced at the coil output is equal to (1).

$$v_{out} = -\frac{d\psi}{dt} = -M\frac{di}{dt} \quad (1)$$

where:

v_{out} is the output voltage.

Ψ is the total flux enclosed by the coil.

M is the mutual inductance between the primary and the secondary windings.

i is the primary current.

t is the time.

Mutual inductance, *M*, is determined by the physical dimensions of the coil and can, for most configurations, be calculated analytically as a closed-form expression. As long as the coil dimensions (winding density, contour length, and volume enclosed by the coil turns) are kept constant, mutual inductance remains constant, thus ensuring constant transducer gain. The exact path of the contour can vary, thus leading to a very popular flexible Rogowski coil implementation.

III. Rogowski Coil Model Development

Similar to the conventional CT, a Rogowski coil can be represented with an equivalent circuit, as shown in Fig. 4, which is very familiar to power engineers.

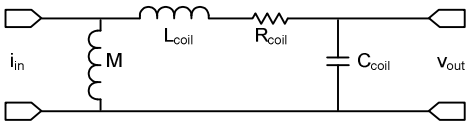

Fig. 4. Rogowski coil equivalent circuit.

Fig. 4 shows great similarity to the equivalent circuit representation of the conventional (magnetic core-based) CT. This is quite normal, given the fact that the main difference between the two is the presence (or absence) of the ferromagnetic core. The behavior of the two, however, is very different due to a large change in individual component values (spanning several orders of magnitude).

In the case of conventional CTs [3], the element in the position of inductor *M* is the CT magnetizing branch inductance, which is typically very large (several henries), while the elements in place of L_{coil}, R_{coil}, and C_{coil} (representing transformer leakage inductance, secondary winding resistance, and winding capacitance, respectively) are typically very small, to the point of being neglected in most models.

In the case of the Rogowski coil, *M* is very small (typically several microhenries), while the coil leakage inductance (L_{coil}) and the coil winding resistance (R_{coil}) are relatively large (several millihenries and 10 to 100 Ω). Winding capacitance is normally distributed but is often approximated with a single capacitor (C_{coil}), which determines (in combination with L_{coil}) the Rogowski coil self-resonance.

The equivalent circuit model is very useful for designing the electronic circuits necessary to process Rogowski coil signals. Model component values can be entered into a SPICE circuit simulator, allowing easy evaluation of the proposed circuit behavior. Following procedure documents, an easy method for determining the required model parameters is as follows:

- Mutual inductance, *M*, is determined by measuring coil sensitivity (mV/A) at a known frequency (e.g., 60 Hz). Simply calculate the inductance that will result in the same voltage drop.
- Leakage inductance is measured directly by using an impedance analyzer.
- Coil winding resistance is measured directly by using an ohmmeter.
- Winding capacitance can be estimated by finding the first resonance peak in the coil output, taking into account any capacitance introduced by the output voltage measurement instrument. A high-impedance oscilloscope probe is often appropriate for the task. Capacitance is calculated so that it resonates at the same frequency when connected in parallel with the previously measured R_{coil}, L_{coil}, and *M*.

Fig. 5 illustrates a typical underdamped coil response causing undesirable ringing associated with fast current transients. Fig. 6 further explains this ringing by presenting the coil response as a function of frequency. It is easy to see that the coil output (voltage drop across *M*) increases with frequency until it reaches the coil self-resonance. Beyond the resonance peak, the coil output rapidly decreases. Fig. 7 shows an appropriately damped impulse response that can be achieved by adding carefully selected loading components. Resistor R3 typically has a dual function, helping with both high-frequency damping and temperature compensation control. With the damping component values shown in Fig. 7, the example coil bandwidth exceeds 80 kHz.

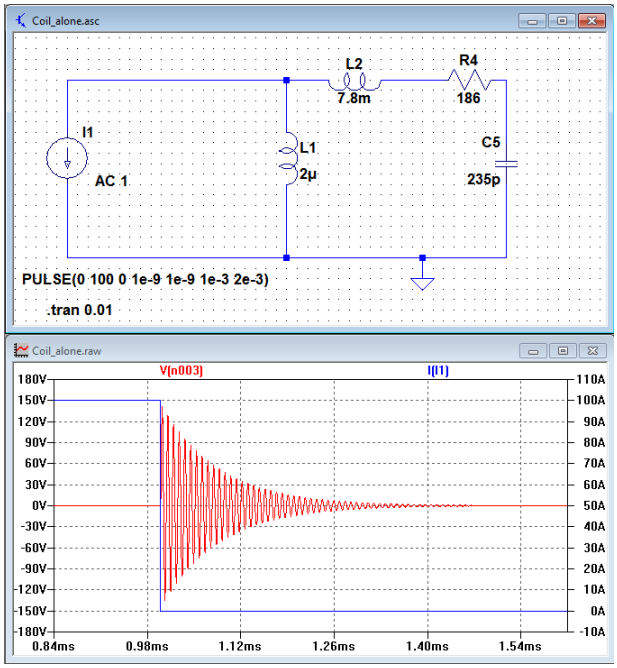

Fig. 5. SPICE simulation illustrating coil resonance effects (response to a fast current transient simulated for a typical low-voltage coil design).

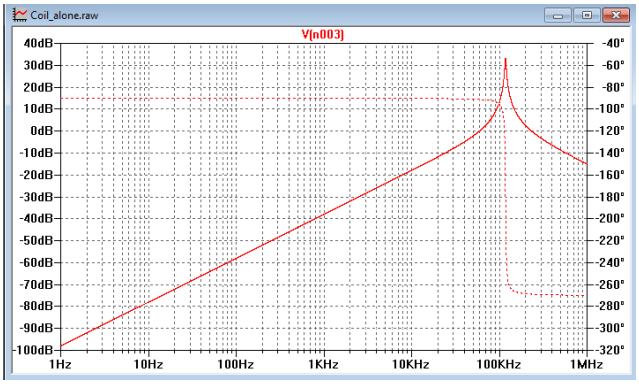

Fig. 6. SPICE simulation illustrating coil resonance effects in the frequency domain.

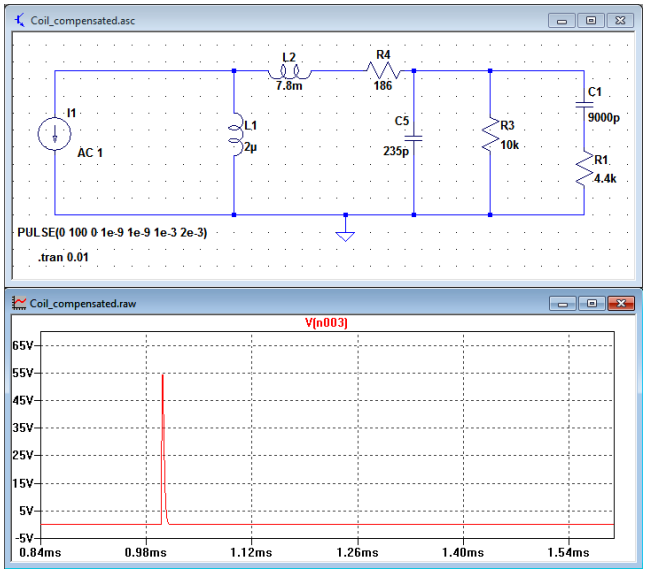

Fig. 7. SPICE simulation illustrating fully damped coil response.

IV. Application Considerations

When compared with conventional (magnetic core-based) CTs, Rogowski coils offer a number of distinct advantages. As with any technology, there are also limitations that must be carefully considered by taking into account specific coil applications. The major advantages and disadvantages are summarized in Table I.

TABLE I
ROGOWSKI COIL ADVANTAGES AND LIMITATIONS

Advantages	Limitations
No saturation, linear, and not affected by dc.	Coil resonance.
Electrically safe when open.	Low sensitivity and shielding.
Potential for lower cost.	Temperature stability.
Smaller size and lower weight.	Integrator implementation.
Wide dynamic range.	Low-frequency noise magnification.
Very low primary burden.	Conductor position sensitivity, limited external field rejection, and manufacturing tolerance.
No magnetizing current error.	Inability to drive multiple loads.

Most of the advantages and disadvantages come from the elimination of the iron core. The advantages are well understood and include the elimination of the core saturation effect as well as immunity to direct current flowing through the primary circuit. If no ferromagnetic materials are present in the vicinity of the coil (this applies to the core, mounting hardware, and shielding components), the coil output is absolutely linear and faithfully represents the primary current [4].

A. Dynamic Range

The Rogowski coil dynamic range is limited primarily by the associated electronics, with the lowest measurable current determined by the combination of coil sensitivity and thermal noise. The highest measurable current is limited by the electronic circuit. Thermal noise is determined by the coil resistance (R4 in Fig. 5) and the coil temperature. It can be calculated in accordance with (2).

$$v_n = \sqrt{4k_B TR} \tag{2}$$

where:

v_n is voltage noise spectral density (V/√Hz).

k_B is Boltzmann's constant ($1.38 \cdot 10^{-23}$ J/K).

T is the absolute temperature (K).

R is the coil resistance.

Thermal noise is typically very low. For the coil shown in Fig. 5 operating at room temperature (300 K), thermal noise is equal to 1.76 nV/√Hz. Assuming 10 kHz bandwidth, this translates to a total noise of 176 nVrms on the coil secondary. Equivalent noise level on the primary will depend on the coil sensitivity. Assuming a typical sensitivity of 200 µV/A at 60 Hz, the primary noise is in the order of 0.88 mA rms. These calculations are rough and do not take into account favorable integrator effects, but they are sufficient to show that Rogowski coils can be used to measure current in both the

power system primary (1 kA to 100 kA) and the power system secondary (1 A to 5 A nominal) currents.

When used in practice, environmental noise and capacitive coupling produced by the neighboring high-voltage conductors are often predominant factors capable of overpowering thermal noise. Careful shielding can be employed to mitigate these effects.

B. Temperature Stability

Conventional CTs are inherently insensitive to temperature variations. The transformer ratio is determined by the number of turns wound around the ferromagnetic core, which, once manufactured, does not change. There are therefore no aging or temperature-related effects. This fact can easily be noticed by inspecting various CT standards, which simply remain mute with regard to such effects [5]. The output of electronic instrument transformers, including low-power current sensors such as Rogowski coils [6], however, shows a complex dependence on temperature that must be carefully addressed by the sensor designer. Fig. 8 shows typical results measured on two Rogowski coil prototypes. The top graph shows the chamber temperature (temperature varied from –45° to +85°C), while the lower graph compares an uncompensated and compensated coil output error measured over a 40-hour period.

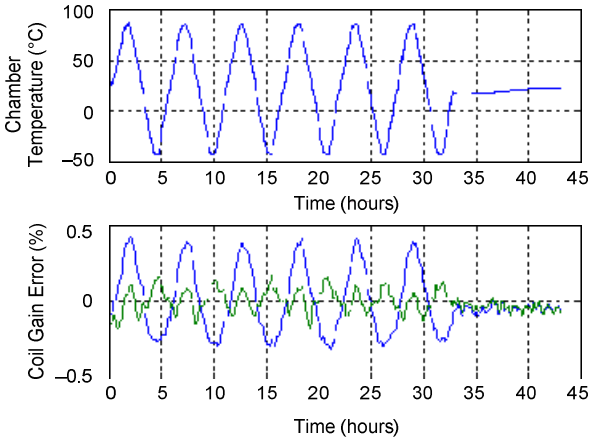

Fig. 8. Rogowski coil gain change with temperature. (Top: Test chamber temperature. Bottom: Compensated versus uncompensated coil gain error.)

Plotting the output of the two coils as a function of temperature allows us to analyze this dependence. By inspecting Fig. 9, it is easy to notice that the uncompensated coil shows mostly linear dependence with a temperature coefficient in the order of +55 ppm/°C. This results in a sensitivity variation in the order of ±0.35 percent over the –45° to +85°C range.

The temperature stability of the Rogowski coil is determined by the thermal expansion coefficient of the nonmagnetic (structural) core material. Careful material selection can minimize these effects, as reported in [7]. However, as long as the coefficient of thermal expansion is linear over the desired temperature range, increased coil output at high temperatures caused by core expansion can be compensated for with a simple loading resistor [6]. This compensation method uses the fact that the copper conductors used to build the coil also change their resistance as a function of temperature. The temperature coefficient of resistivity for copper is in the order of 3,900 ppm/°C, allowing a very small load (large burden resistor) to counteract the small gain variations produced by the coil.

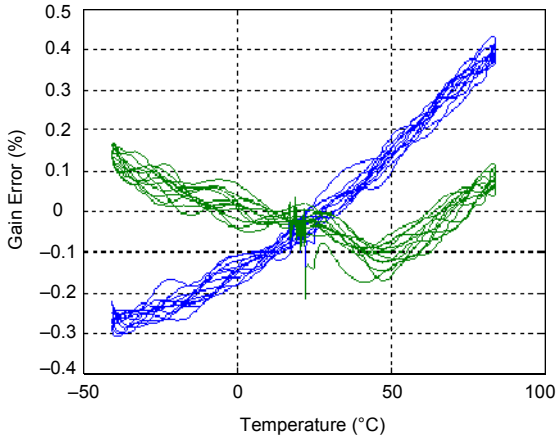

Fig. 9. Gain error as a function of temperature (compensated coil shown in green versus uncompensated coil shown in blue).

Fig. 8 and Fig. 9 also show results for a compensated Rogowski coil. It can be seen that the simple addition of the burden resistor reduces the temperature variation from ±0.35 to ±0.15 percent.

The results in Fig. 9 include gain variations contributed by the analog-to-digital (A/D) converter and the associated A/D converter reference, thus reflecting the total stability achieved by a Rogowski coil-based data acquisition system. As reported in [2], carefully designed Rogowski coils with temperature compensation can achieve and maintain a 0.1 percent accuracy class over a wide temperature range.

C. Integrator Design

As shown in [1], Rogowski coils produce output voltage that is proportional to the rate of change (derivative) of the primary current. Most applications, including revenue metering, power quality measurements, and protection, expect to use primary current, which in most applications makes it necessary to perform signal integration [2].

Integration can be performed by using an analog circuit (often called an integrator) or digitally by using a signal processing algorithm. In its simplest form, an integrator is a first-order low-pass filter with a response that compensates for the frequency-dependent gain increase illustrated in Fig. 6. (straight, upward-sloping line to the left of the resonance peak).

Fig. 10 shows a typical block diagram illustrating the two integrator implementation methods. The top part of the figure shows an analog integrator followed by the A/D converter, while the lower part uses a digital signal processing algorithm to perform integration. A digital signal processing approach provides better stability and repeatability among multiple channels (integrator response that is not affected by circuit component variations), while the analog integrator circuit may have advantages in terms of signal clipping and the processing of fast transients. Additional details describing integrator behavior follow.

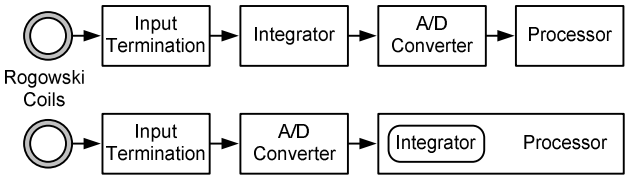

Fig. 10. Data acquisition circuit topologies.

Fig. 11 illustrates the basic integrator operation, with the top graph showing primary current (in this case, simulated fully offset fault waveform with X/R = 40), the middle graph showing coil output voltage (shifted by 90 degrees and showing significant dc component attenuation), and the bottom graph showing the integrator output.

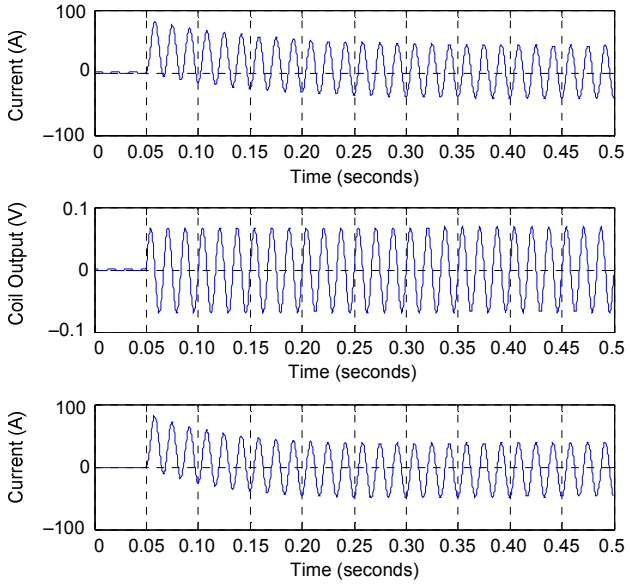

Fig. 11. Rogowski coil output integration process. (Top: Fully offset fault current. Middle: Rogowski coil output. Bottom: Integrator output.)

Careful comparison of the input current with the integrator output reveals that the 60 Hz waveform was fully restored with the correct phase angle, but the decaying low-frequency (dc offset) exponential was shortened. While the difference is present in Fig. 11, it is too small to notice and is shown further in Fig. 12.

This type of behavior is common to all real-life implementations. It is caused by the fact that practical systems cannot afford to implement the infinite dc gain that would be required to faithfully reproduce the dc component. Even if such gain were available, the dc component measurement would depend on precise knowledge of initial system conditions. To make things worse, all electronic systems introduce a small amount of error, such as an operational amplifier dc offset error, which accumulates, thus driving the ideal integrator into saturation. To eliminate these problems, all practical systems have some means of reducing the integrator gain at low frequencies. Translated to the overall system frequency response, this reduction shows as a high-pass filter with the corner frequency typically located somewhere between 0.1 and 1.0 Hz.

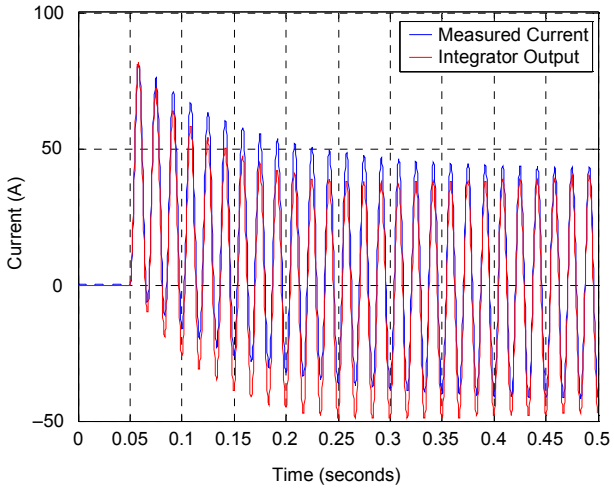

Fig. 12. Low-frequency cutoff effects.

The immediate questions that come to mind are what is the best value for this cutoff frequency and how does it compare to a conventional CT response? To answer these questions, we performed measurements on auxiliary CTs used by three mainstream relay manufacturers. Measurements were performed with a fully offset test waveform (X/R = 40) supplied to inputs rated for 1 A nominal. The results are shown in Fig. 13.

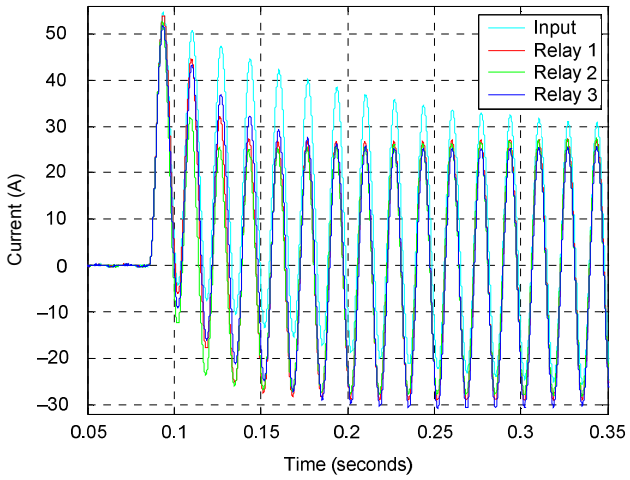

Fig. 13. Low-frequency behavior of conventional relay CTs with a 20 A fully offset fault current.

Surprisingly enough, all three tested relays showed similar behavior, with the conventional auxiliary CT response being similar to the Rogowski coil-based system shown in Fig. 12. Auxiliary CTs used in the tested relays do not exhibit hard saturation effects at X/R = 40, with exponential decay being simply shortened by the increased magnetizing branch leakage. Gradual (graceful) entry into saturation hints at the presence of the core gap, which, in these particular designs, was accomplished through CT core construction (all three relays use EI core laminations resulting in a distributed air gap).

It is interesting to note that the standard requirements for primary instrument transformers (and the associated IEC 60044 standard series) provide strict limits governing the instrument transformer dynamic response [5]. In accordance with the stated accuracy classes (5P and 10P), primary transformers are required to keep the maximum peak instantaneous error below 10 percent. This requirement results in conservative designs, with an exceptionally good transient response and a significant safety margin guarding against saturation. In short, conventional instrument transformers used in high-performance transmission applications provide high-quality signals to the associated secondary equipment.

To make things more interesting, the same method (peak instantaneous error described in IEC 60044) can be used to evaluate the auxiliary relay CT response. Detailed results applicable to one of the tested relays are shown in Fig. 14.

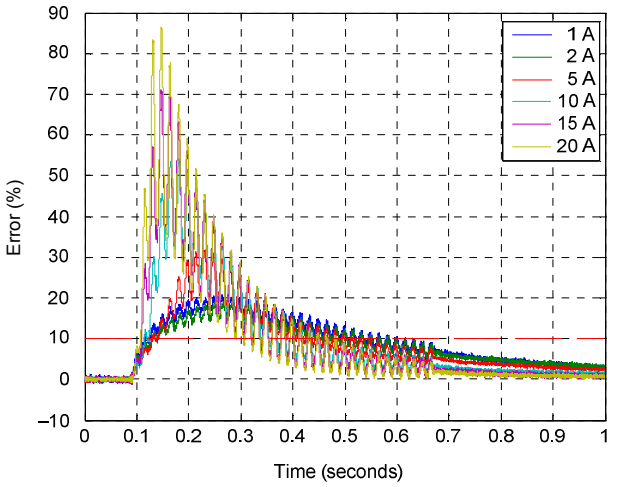

Fig. 14. Instantaneous error as a function of fault current level derived in accordance with [5] (1 A inputs, X/R = 40).

The first surprise is the apparent error magnitude. While the primary CTs are capable of reproducing exponential dc transients with a 10 percent error (limit shown with the dashed red line), the auxiliary relay CTs appear to simply discard that information, making it invisible to the relay.

Further analysis revealed that the auxiliary CT response measured on the three relays can be closely approximated with a first-order high-pass filter with a cutoff frequency that depends on the fault current level. Once presented this way, conventional CT response can be easily compared with the electronic instrument transformer requirements described in [5].

Table II shows the results of the first-order model performed for one of the relays.

TABLE II
CONVENTIONAL CT CUTOFF FREQUENCY EXAMPLE

Fault Current Level	1 A	2 A	5 A	10 A	15 A	20 A
Corner Frequency	0.5 Hz	0.42 Hz	0.7 Hz	1.9 Hz	2.5 Hz	3 Hz

The results are eye-opening and can be summarized with an oversimplified statement: primary CTs provide excellent reproduction of the low-frequency current waveforms, but the protective relays do not typically use it. This is quite normal given the fact that many relaying algorithms go to exceptional lengths to eliminate the undesirable effects the dc offset has on the Fourier or cosine filter-based phasor estimates.

Reference [5] also introduces a special accuracy class (5TPE) designed specifically for electronic instrument transformers with a built-in high-pass filter. To satisfy the 10 percent error requirement for X/R = 40, the filter cutoff frequency needs to be the in the order of 0.1 to 0.15 Hz. This requirement was set to ensure a good match between the conventional and electronic CTs.

When it comes to Rogowski coil integrators, the high-pass filter cutoff frequency can be conveniently set anywhere between 0.1 and 1.0 Hz. A lower frequency setting brings the coil performance in line with the primary CT standards, while a higher frequency setting brings it closer to the mainstream relays. The final choice depends on the application and is presently being investigated by the International Electrotechnical Commission Technical Committee 38, Working Group 37 (IEC TC38, WG37) for inclusion in the new standard IEC 61869-13: Instrument Transformers – Part 13: Standalone Merging Unit, which is under development.

D. Application of Rogowski Coil Technology to Secondary Circuits

Regardless of the voltage level, Rogowski coils are normally used to measure current at the power system primary. The maximum short-circuit current that can flow in the primary is normally determined by the source impedance, which, in the case of the power system, is mostly inductive. Fault current magnitude is determined by the source inductance, which, in effect, limits the maximum rate of change of the current. This fact allows for easy calculation of the Rogowski coil maximum output voltage that will be present during short-circuit faults.

However, can the Rogowski coil be used to measure the conventional instrument transformer secondary circuit, and what is the maximum voltage that can be expected in that case? As it turns out, as long as the conventional instrument transformer remains linear, the rate of change of the short-circuit current remains unchanged, faithfully reflecting primary circuit characteristics. Things change, however, if the conventional CT core becomes saturated. Fig. 15 shows an

example secondary waveform exhibiting significant CT saturation. Saturation was caused under laboratory conditions by using an excessive burden and undersized CT core but can nevertheless be considered representative of the demanding, cost-constrained industrial applications in which such cores are often used.

A simple inspection of Fig. 15 shows that the rate of change of the current is significantly increased, with sudden changes occurring at the moment the CT core goes into saturation (CT output collapses).

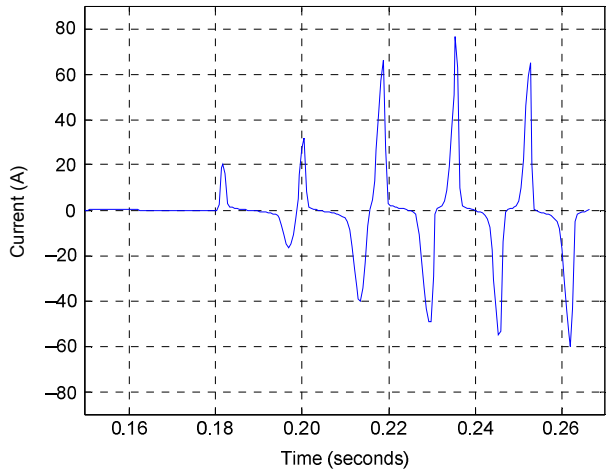

Fig. 15. Fault current waveform produced by a heavily saturated CT.

The saturated waveform derivative produced by the waveform in Fig. 15 is shown in Fig. 16. The waveform exhibits large peaks with a maximum determined by the CT leakage inductance.

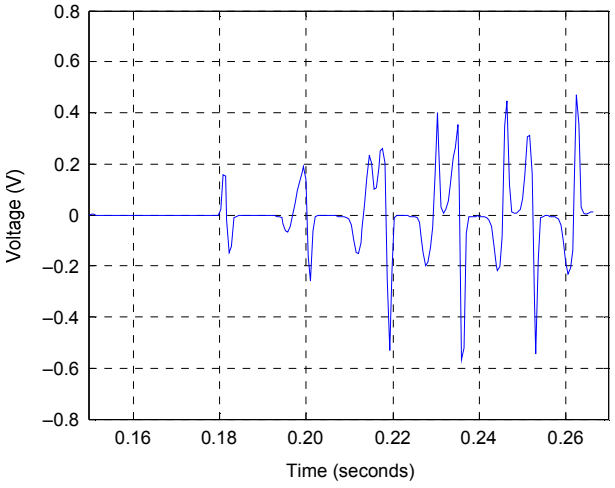

Fig. 16. Rogowski coil output responding to the signal in Fig. 15 (output voltage magnitude is arbitrary and determined by coil sensitivity).

The integrator response to such a distorted waveform depends on the electronic input circuit design and the data acquisition system architecture employed (see Fig. 10). Caution is required with systems that use digital filter-based integrators or employ analog preamplifier circuits or integrator implementations, which may clip some of the peaks, as shown in the Fig. 17 example. A similar problem can be caused by external surge suppression components or lightning arrestors, which may be used in the input circuit.

Analog integrators with the Rogowski coil signal fed directly to an integrating capacitor (active or passive) do not have this problem and can faithfully reproduce the input current regardless of the shape of the curve. They can satisfy even the most demanding power system applications, including those requiring faithful preservation of the input waveshape (CT saturation signature).

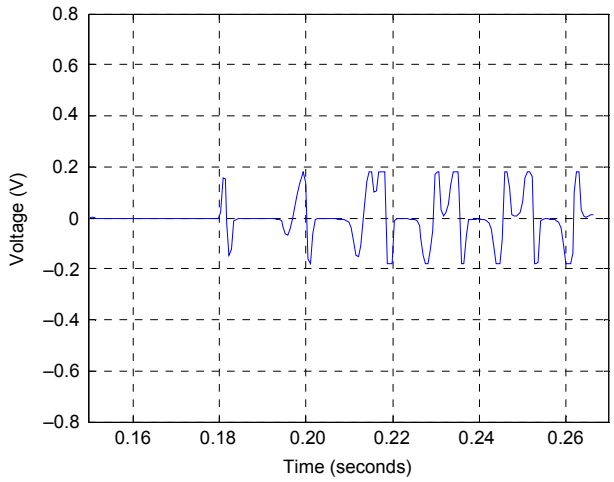

Fig. 17. Rogowski coil peak-clipping example (illustration only, shows arbitrary clipping level).

E. Digital Integrator Implementation

The digital integrator implementation approach, shown on the bottom of Fig. 10, offers exceptional stability over temperature, is resilient to electromagnetic interference, and ensures precise matching among multiple channels, but it may be exposed to signal clipping (finite A/D converter range).

Fig. 18 shows what happens if the clipped waveform is processed with a simple first-order integrator algorithm that has not been optimized to deal with clipping-induced input errors.

It is interesting to note that the integrator output waveshape remains somewhat similar to the original input current. Unfortunately, asymmetric clipping of the input waveform causes the integrator to lose track of the dc component. As shown in Fig. 18, the dc error starts to accumulate, leading to integrator runaway with a total loss of zero crossings and the eventual saturation of the integrator.

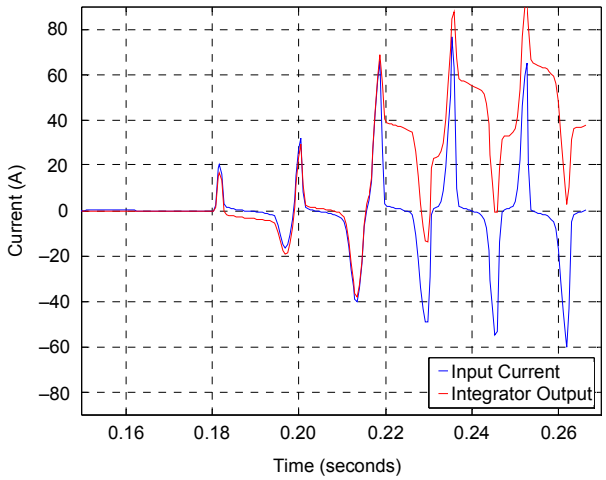

Fig. 18. Simple integrator algorithm example showing typical response to clipped waveform input.

In the case when the A/D converter is followed by a numeric integration algorithm (bottom part of Fig. 10), integrator runaway can be alleviated by adding dc component stabilization logic. Stabilized results obtained by dynamically adjusting the high-pass filter time constant are shown in Fig. 19. Although not ideal, the stabilized integration algorithm was capable of restoring the current waveform zero crossings and retained most of the rms energy present in the original waveform. A restored waveform allows the use of conventional protection elements, including the well-known distortion index-based peak detector element used to address primary CT saturation [8].

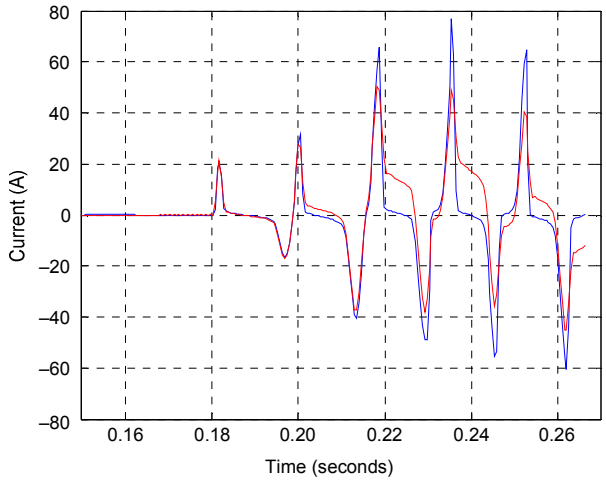

Fig. 19. Example of dc-stabilized integrator algorithm showing response to clipped waveform input.

Single-cycle rms current magnitude as a function of clipping level is shown in Fig. 20. The blue trace shows the rms current magnitude contained in the original current waveform, while the succession of red traces shows what happens if the clipping level in Fig. 17 is varied between 0.18 V (heavy clipping) and 0.4 V (minimum clipping).

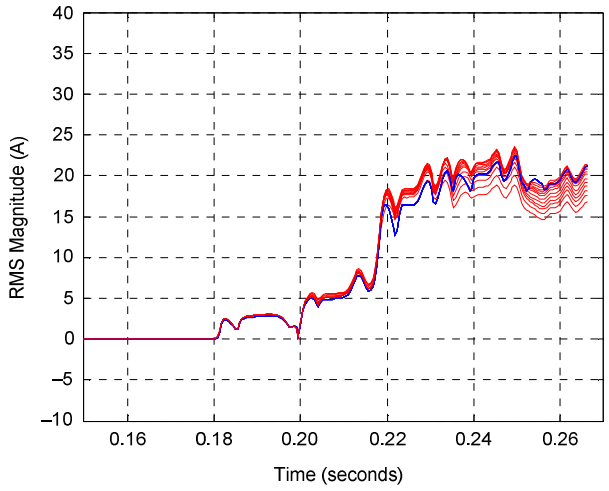

Fig. 20. Single-cycle rms current magnitude as a function of clipping level.

Given the amount of clipping involved, it is interesting to note that the stabilized integrator algorithm remains stable, degrades gracefully, and is reasonably close to the original input waveform. Obviously, as the primary CT saturation worsens, all algorithmic methods used to mitigate that saturation eventually fail, further supporting the need for proper CT sizing in protection system applications. The stabilized integrator approach is very stable, allowing the digital integrator to be used in overcurrent relay applications. More demanding applications relying on precise reconstruction of the input waveform should consider using the analog integrator implementation.

F. Low-Frequency Noise Considerations

As a first-order low-pass filter, the integrator is very good at reducing the high-frequency input noise generated by the A/D converter or the input amplifier circuitry. However, depending on the Rogowski coil gain, this often means that the integrator also accentuates low-frequency noise. This behavior is shown in Fig. 21, which shows input noise density recorded on the system using an A/D converter followed by the digital integrator.

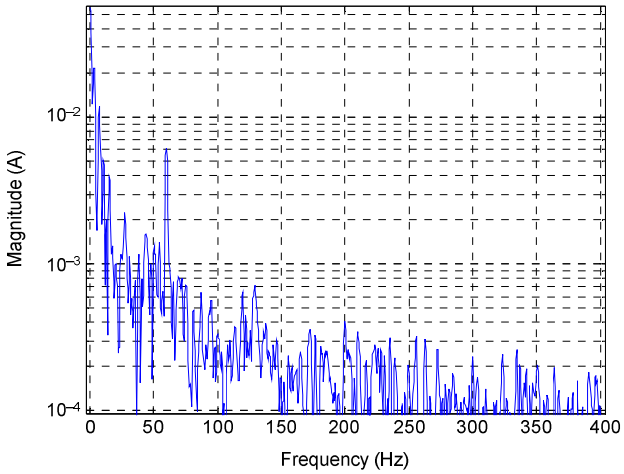

Fig. 21. Integrator output noise density as a function of frequency for an A/D converter-based data acquisition chain with a digital integrator (example).

The noise amplification level is also linked to the high-pass filter cutoff frequency explained previously. The selection of an excessively low corner frequency (for example, 0.1 Hz instead of 1.0 Hz) results in a tenfold noise increase at the corner frequency. This type of concern is especially present in high-precision metering applications where low-frequency noise energy has the potential of reducing overall system accuracy.

With their exceptional linearity, Rogowski coils promise to join the long-separated metering and protection accuracy classes, with low-frequency noise performance remaining one of the lone-standing obstacles of this goal. Low-frequency noise presents no problems to typical protection applications, with the only consequence being visual noise presence that can be observed in low-current COMTRADE reports.

G. Position Sensitivity and External Field Rejection

The high-quality Rogowski coil geometry is normally insensitive to external magnetic fields and the position of the primary conductor within the coil. Unfortunately, practical realization of such geometry results in limited rejection of the external magnetic field. References [1], [2], and [9] provide additional details about practical coil construction. External field rejection depends on the manufacturing tolerances and is normally constant for a given design. As long as the core is not driven to saturation, conventional CTs will typically show better rejection of the external magnetic fields. Care is required to properly describe Rogowski coil external field rejection properties so that they do not become a factor in the intended power system application.

H. Relay Interface

Rogowski coils can be built into products or designed as standalone current sensors [5] [10] [11]. Reference [10] describes a low-energy (200 mV) interface, which is particularly suitable for medium-voltage Rogowski coil applications. Additional standardization efforts are under way within IEC TC38 and are intended to further standardize the low-energy sensor interface in protective relays and the new digital transmission devices called standalone merging units.

I. Implementation Example

For a Rogowski coil implementation example, we consider the case of a simple, low-voltage motor overload relay. Such relays are normally connected to the power system primary and can be exposed to exceptionally high current levels. Depending on the protected motor size, relay continuous full load current may range from several amperes to several thousand amperes [National Electrical Manufacturers Association (NEMA) sizes 00 to 9]. Motor starting currents are typically 6 to 6.5 times higher (NEMA B design) but can in some designs exceed 10 times the continuous full load current.

A motor overload relay is especially appropriate for Rogowski coil applications. It can take advantage of an exceptionally wide dynamic range, low coil weight, and the flexibility offered by configurable coil shapes. When compared with conventional heating elements, Rogowski coils are virtually insensitive to excessive current levels and can easily achieve IEC Type 2 coordination. When necessary, a Rogowski coil-based overload relay can be fed by a 5 A CT secondary, further enhancing overall design flexibility.

Fig. 22 shows a Rogowski coil-based data acquisition system example optimized for NEMA sizes 00 to 4 motor overload relay applications. The example uses A/D converter gain switching and is capable of correctly digitizing signals up to 2,000 A rms, as well as operating from a 5 A auxiliary CT secondary.

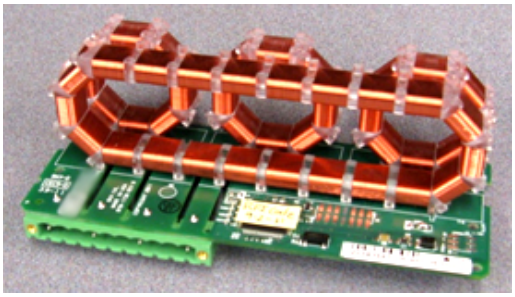

Fig. 22. Three-phase Rogowski coil data acquisition system example.

V. CONCLUSION

This paper discusses the practical considerations of using Rogowski coils in modern protective relays. It explains the advantages and some of the potential pitfalls that need to be addressed. This paper also discusses data acquisition chain architecture options, explains clipping effects associated with certain architectures, and, for the first time, explores the possibility of using Rogowski coils in secondary relay circuits fed by conventional CTs.

VI. REFERENCES

[1] IEEE Standard C37.235-2007, IEEE Guide for the Application of Rogowski Coils Used for Protective Relaying Purposes.

[2] IEEE PSRC Special Report, "Practical Aspects of Rogowski Coil Applications to Relaying," September 2010. Available: http://www.pes-psrc.org.

[3] IEEE Standard C57.13-2008, Requirements for Instrument Transformers.

[4] B. V. Djokic, J. D. Ramboz, and D. E. Destefan, "To What Extent Can the Current Amplitude Linearity of Rogowski Coils Be Verified?," *IEEE Transactions on Instrumentation and Measurement*, Vol. 60, Issue 7, July 2011, pp. 2409–2414.

[5] IEC 60044-8, Instrument Transformers – Part 8: Electronic Current Transformers, 2002.

[6] D. A. Ward, "Precision Measurement of AC Currents in the Range of 1 A to Greater Than 100 kA Using Rogowski Coils," proceedings of the British Electromagnetics Measurement Conference, National Physical Laboratory, October 1985.

[7] J. D. Ramboz, "Machinable Rogowski Coil, Design, and Calibration," *IEEE Transactions on Instrumentation and Measurement*, Vol. 45, Issue 2, April 1996, pp. 511–515.

[8] G. Benmouyal and S. E. Zocholl, "The Impact of High Fault Current and CT Rating Limits on Overcurrent Protection," proceedings of the 29th Annual Western Protective Relay Conference, Spokane, WA, October 2002.

[9] L. A. Kojovic, M. T. Bishop, and T. R. Day, "Operational Performance of Relay Protection Systems Based on Low Power Current Sensors," proceedings of the 36th Annual Western Protective Relay Conference, Spokane, WA, 2009.

[10] IEEE Standard C37.92-2005, IEEE Standard for Analog Inputs to Protective Relays From Electronic Voltage and Current Transducers.

[11] L. A. Kojovic, "Comparative Performance Characteristics of Current Transformers and Rogowski Coils Used for Protective Relaying Purposes," proceedings of the IEEE PES General Meeting, Tampa, FL, June 2007.

VII. BIOGRAPHIES

Veselin Skendzic is a principal research engineer at Schweitzer Engineering Laboratories, Inc. He earned his B.S. in electrical engineering from FESB, University of Split, Croatia; his Master of Science from ETF, Zagreb, Croatia; and his Ph.D. degree from Texas A&M University, College Station, Texas. He has more than 25 years of experience in electronic circuit design and power system protection-related problems. He is a senior member of the IEEE, has written multiple technical papers, and is actively contributing to IEEE and IEC standard development. He is a member of the IEEE Power Engineering Society (PES) and the IEEE Power System Relaying Committee (PSRC) and a past chair of the PSRC Relay Communications Subcommittee (H).

Bob Hughes received his B.S. in electrical engineering from Montana State University in 1985. He is a senior marketing engineer in the protection systems department at Schweitzer Engineering Laboratories, Inc. Bob has over 20 years of experience in electric power system automation, including SCADA/EMS, distribution automation, power plant controls, and automated meter reading. He is a registered professional engineer and a member of IEEE.